

RIGA TECHNICAL UNIVERSITY
Faculty of Power and Electrical Engineering
Institute of Power Engineering

Julija MAKSIMKINA

Student of the Doctoral Program “Electrical Machines and Apparatus”

**INVESTIGATION OF THE DYNAMIC MODES OF HIGH POWER
INDUCTION MOTORS, TAKING INTO ACCOUNT THE SKIN EFFECT**

Summary of Doctoral Thesis

Scientific supervisor
Dr. habil. sc. ing., professor
I. RAŅĶIS

RTU Press
Riga 2015

Maksimkina J. Investigation of the Dynamic Modes of High Power Induction Motors, Taking into Account the Skin Effect. Summary of Doctoral Thesis. –R.: RTU Press, 2015.–35 p.

Printed according to the decision of RTU Institute of Power Engineering as of 04. 09. 2015, Minutes No. 56.

I express my deep gratitude to my Doctoral Thesis's first supervisor assoc. prof. **Andrejs Zviedris** for the definition of interesting research topic and introduction to the procedure of elaborating the Doctoral Thesis.

I express my sincere gratitude to prof. **Ivars Raņķis** for work management.

I express my deep gratitude to prof. **Kārlis Ketners** for the consultations and valuable assistance offered in the issues of modeling in the non-stationary regimes of induction motors.

I express my deep gratitude to lect. **Uldis Brakanskis** for valuable assistance offered in the designing and research issues of induction motors.

ISBN 978-9934-10-756-6

**DOCTORAL THESIS
PROPOSED TO RIGA TECHNICAL UNIVERSITY
FOR THE PROMOTION TO THE SCIENTIFIC DEGREE OF DOCTOR
OF ENGINEERING SCIENCE (DR. SC. ING.)**

To be granted the scientific degree of Doctor of Engineering Science, the Doctoral Thesis has been submitted for the defence at the open meeting on 17. of December 2015 at 14.00. at the Faculty of Power and Electrical Engineering, Riga Technical University, Azenes Str. 12 k-1, 212. Room.

OFFICIAL REVIEWERS

Leading Researcher, *Dr. habil. sc. ing.* Vladislavs Pugačevs
Latvian Academy of Sciences, Institute of Physical Energetics, Latvia

Professor, *Dr. sc. ing.* Aleksandrs Gasparjans
Latvian Maritime Academy, Latvia

Professor, *Dr. habil. sc. ing.* Algirdas Smilgevičius
Vilnius Gediminas Technical University

DECLARATION OF ACADEMIC INTEGRITY

I hereby declare that the Doctoral Thesis submitted for the review to Riga Technical University for the promotion to the scientific degree of Doctor of Engineering Science is my own and does not contain any unacknowledged material from any source. I confirm that this Thesis has not been submitted to any other university for the promotion to other scientific degree.

Julija Maksimkina(Signature)

Date:

The Doctoral Thesis has written in the Latvian language. It contains introduction, 4 chapters, conclusions and main results of the research. The total volume of the Thesis is 128 pages. The Thesis consists of 61 figures and 18 tables. The number of references used in the Thesis is 130.

TOPICALITY OF THE RESEARCH

The present research and a large number of recent scientific articles [3], [4], [6], [11]–[15] testify that it is important to carry out operative calculation of induction motor parameters today. In the existing studies, there is not a rigorous analytical solution to evaluate the impact of the skin effect on the rotor resistances and inductance. Numerous independent calculation methods have been created; each has its own characteristics and capabilities, as well as disadvantages. Therefore, the correct calculation method of induction motors with variable parameters, which depend on rotor electromagnetic process during the dynamic processes, has not been created [24], [40], [41].

The research methods of electrical motors are continuously expanding and evolving. The used methods for quality improvement can be achieved only on the basis of modern computer technology widespread application. The mathematical model correctly performed by the computer can be considered the most universal research tool. This model provides a solution to a variety of tasks; the consideration of various important factors makes it possible to get an idea of the phenomena, which mainly correspond to processes, which are observed in the research.

The research into the computer mathematical models of electrical motors opens new perspectives for studies of electrical motors with numerical methods. The physical studies of electrical motors are required for the creation of experimental samples, lead to high financial costs and do not result in the opportunities provided by a computing experiment. The computing experiment is intended to such complicated multiparameter non-linear process research and optimization, to which the application of traditional research methods is too complicated or even impossible. The opportunity to replace the real object with the mathematical model provides greater advantages of electrical motor studies.

Taking into account the above-mentioned considerations, the theme of the Doctoral Thesis about studies of induction motor transient processes with variable rotor parameters under the impact of skin effect in dynamic regimes of motors is topical and important.

OBJECT UNDER INVESTIGATION, AIM OF AND TASKS OF THE RESEARCH

The squirrel-cage induction motor SCIM (high power SCIM) although predominantly with a nominal power exceeding 10 kW is the research **object** of the Doctoral Thesis.

The **aim** of the Doctoral Thesis is, taking into account the impact of the skin effect in rotor, to create and study SCIM mathematical models in static and dynamic modes, which corresponds to modern mathematical modeling capabilities.

To achieve the aim set, the following **main tasks** have been formulated and solved:

1. To create the SCIM mathematical model taking into account the impact of the skin effect.
2. To work out algorithms and programs for determination of variable rotor parameters.
3. To carry out the dynamic calculations of induction motor taking into account the impact of the skin effect in rotor.
4. To verify the reliability of the obtained models and calculations results.

MEANS AND METHODS OF THE RESEARCH

1. The exploration of the theory of the SCIM transient process in order to define research task, aims and methods of solution.
2. The materials of international conferences, as well as the materials of various foreign publications devoted to the impact of skin effect in rotor.
3. The mathematical calculations, using software *MS Excel*, *Fortran*, software complexes *QuickField 5.7* and *Power Simulation (PSIM)*.
4. The mathematical modeling for the calculations of SCIM variable parameters and transient process.

SCIENTIFIC NOVELTY OF THE RESEARCH

In the Doctoral Thesis, the calculation methodology of variable parameters of the squirrel-cage induction motor rotor is developed, taking into account the impact of the rotor skin effects.

PRACTICAL APPLICATION OF THE RESEARCH RESULTS

The computer program proposed by the author makes it possible to calculate the transient process of squirrel-cage induction motor both at rotor constant parameters and in case of different change in the ways of variable rotor parameters during the transient process. The author's proposed methodology can be used not only for the calculation of the rotor parameters of motor, but also for designing of new SCIM with an **arbitrary** rotor slot **configuration**.

THE APPROBATION OF RESEARCH RESULTS

The main results of the research have been presented at the following international conferences:

1. 14th International Symposium "Topical Problems in the Field of Electrical and Power Engineering & Doctoral School of Energy and Geotechnology II", Pernava, Estonia, 13.–18.01.2014.
2. 12th International Scientific Conference "Engineering for Rural Development", Jelgava, 23.–24.05.2013.
3. 8th International Conference on Electrical and Control Technologies, Kaunas, Lithuania, 2.–3.05.2013.
4. 15th International Conference Maritime Transport and Infrastructure, Latvian Maritime Academy, Riga, 25.–26.04.2013.
5. 43rd International Scientific Conference on Power and Electrical Engineering, RTU, Riga, 2002.
6. 42nd International Scientific Conference on Power and Electrical Engineering, RTU, Riga, 11.–13.10.2001.

THE AUTHOR'S PUBLICATIONS

1. Zviedris A., Maksimkina J. Influence of variable parameters of asynchronous drives on the transient// Proceeding of the 3rd Research Symposium of Young Scientists, Actual problems of electrical drives and industry automation, TTU, Tallinn, Estonia, 2001. pp. 50–53.
2. Zviedris A., Maksimkina J., Maņņitko A. Asinhrono dzinēju katalogu datu izmantošana pārejas procesa parametru noteikšanai// Scientific Journal of RTU. Power and Electrical Engineering, 2002. 4. series, 7. iss., pp. 10–16.
3. Звиедрис А., Максимкина Ю. Система алгоритмов для расчета параметров асинхронного двигателя с короткозамкнутым ротором// Proceeding of Elektros energetika ir tehnologijos, KTU, Kaunas, Lietuva, 2004. pp. 195–200.
4. Zviedris A., Maksimkina J. Inventory of different methods of rotor's parameters influence of starting process of induction motor// Scientific Journal of RTU. Power and Electrical Engineering, 2006. 4. series, 18. iss., pp. 45–50.

5. Maksimkina J. The Research of the Processes of the Squirrel-cage Induction Motor's Direct Start-up in the Setting of the Rotor's Variable Parameters// Scientific Journal of RTU. Power and Electrical Engineering, 2012. 4. series, 30. iss., pp. 53–58.
6. Maksimkina J. The Research of the Processes of the Squirrel-cage Various Power Induction Motor's Direct Start-up// Proceeding of International Conference on Maritime Transport and Infrastructure, 2013. p. 18.
7. Maksimkina J. Direct Start-up of the Squirrel-cage Induction Motor at Variable Parameters of the Rotor// Latvian Journal of Physics and Technical sciences, 2013. №1, vol.50, pp. 10–21.
8. Maksimkina J. The Need to Consider the Skin Effect in the Study of Direct Start-up of the Squirrel-cage Induction Motor// Proceeding of International Conference on Electrical and Control Technologies, Technologija, Kaunas, Lithuania, 2013. pp. 106–110.
9. Maksimkina J. Methods for Calculation of the Variable Parameters of a Rotor of the Cage Induction Motor// Proceeding of International Conference on Topical Problems in the Field of Electrical and Power Engineering, Elektrijam, Pärnu (Pernava), Estonia, 2014. pp. 106–111.

CONTENTS

Introduction

1. Methods for Determination of the Variable Parameters of the Rotor in the Transient Mode of Operation
2. The Calculations of the Rotor Variable Parameters with Different Methods
3. Mathematical Models of a Squirrel-Cage Induction Motor and Their Application in the Research of Transition Process with Current Displacement
4. The Calculations of the Transient Process of Induction Motor with Rotor Variable Parameters

Conclusions Future Research

List of References Used in the Summary

INTRODUCTION

At present induction motor is the main electric motor that is used as a drive motor for majority mechanisms (about 90 % of all motors used in national economy are induction motors) [19], [22], [30].

The necessity of continuous security of electricity supply prompted experts to pay attention to short-term transition processes that arise in electrical motors and electrical network in case of starting-up and sudden disturbances of stationary operating mode [16].

A common feature of these processes is that the current and torque values deviate significantly from values (current and torque), which are characteristic for stationary operating mode at the constant rotation speed [10], [17], [26]. In addition, the torques and currents can reach very high values, and in particular unfavorable cases torque value can reach up to 15 times greater than the nominal value and current — 3 times from its steady state value [34], [39], [43].

Researching the transition processes of induction motors, resistance plays a more important role [7], [12], [42]. The reason for this is that resistance plays a more important role in creation of torque, and in the research of transient process it is usually considered to be a constant value during the process [39]. Analyzing the transient process of induction motors at constant rotor resistance during the process, only qualitative picture can be obtained, which often, particularly with regard to torque, may prove to be incorrect.

In order to achieve good efficiency, the induction motors must operate at rated (nominal) load with a small slip value ($s_N = 0.02 - 0.05$) and, thereby, they must have a high stiffness of mechanical characteristics ($s_N = 0.06 - 0.15$) provided by the small rotor resistance [47]–[49]. This request for the induction motors with constant parameters is contrary to the requirements of sufficient start-up motor torque value, because induction motor start-up torque increases with an increasing rotor resistance. But, if the corresponding stationary mode rotor parameters are saved, the motor starting torque with such rotor winding resistance will be significantly less than the nominal one [20], [32]. This eliminates the possibility to run the following motors with constant and close to the rated load. Starting motors with a small load, the torque curve distortion could cause difficulties due to the impact of higher field harmonics. In this context, the motors of general meaning have been constructed only as motors with variable parameters [28], [29]. In order to increase the rotor resistance R_2 , and, thereby increase the torque M_p at start-up, the phenomenon of skin effect or current displacement effect is used. This problem is solved, using the rotor winding special constructions [6], [19], [40], [41]. It should be noted that the rotation speed curve of induction motors is also dependent on rotor inductance during the transition

process [5], [15], [42]. In order to make the correct induction electric drive dynamic calculations, **it is necessary to take into account the rotor parameter changes** at different slip values during the process.

The **aim** of the Doctoral Thesis is, taking into account the impact of the skin effect in rotor, to create and study SCIM mathematical models in static and dynamic modes, which corresponds to modern mathematical modeling capabilities.

To achieve this aim, the following **main tasks** have been formulated and solved:

1. To create the SCIM mathematical model taking into account the impact of the skin effect.
2. To work out algorithms and programs for determination of variable rotor parameters.
3. To carry out the dynamic calculations of induction motor taking into account the impact of the skin effect in rotor.
4. To verify the reliability of the obtained models and calculations results.

The first chapter reviews various existing methods, as well as the author's proposed methodology with due account for the rotor skin effect of induction motor in the dynamic processes.

In the second chapter, based on the proposed methods, the calculation of rotor variable parameters is carried out, the comparative analysis of the calculation results is shown, the possibility of different method application and their calculation accuracy are evaluated.

The third chapter describes the mathematical model of squirrel-cage induction motor with variable parameters of the rotor, as well as provides the dynamic process calculation algorithm and software description.

The fourth chapter is dedicated to experimental research for dynamic process of induction motor with variable rotor parameters.

1. METHODS FOR DETERMINATION OF THE VARIABLE PARAMETERS OF THE ROTOR IN THE TRANSIENT MODE OF OPERATION

It is known [5], [17], [19] that at start-up of the squirrel-cage induction motor, when the frequency of the rotor is high ($f_1 = f_2$), the rotor bar current is forced out of the air gap direction that, in essence, is the expression of the skin effect in conductors. At start-up of the squirrel-cage induction motor, only the upper part of the rod actively works and its working cross-section area decreases, which causes R_2 to increase. Simultaneously with the current displacement the rod inductance is reduced, which together with increasing R_2 leads to the increase in starting torque.

During the start-up of motor, the current frequency of the rotor is reduced. When the motor reaches the rated speed, the current frequency of the rotor is very low ($f_2 = sNf_1 \leq 1 - 5$ Hz). In this case, the effect of current displacement practically disappears, and the current is distributed evenly over the cross section of the rod. Rod resistance becomes small, and the motor runs with a good efficiency.

1.1. Detection of the Rotor Parameter Changes of Motor Dependent (the Impact of Skin Effect) Studied Range

In order to identify the need to consider the skin effect at start-up, the electromagnetic torque of wide range of A4 SCIM was calculated with $p = 2$ [32] starting torque and nominal torque relations M_{start}/M_N at different frequencies f_1 of supply voltage at $s = 1$ and the evaluation of necessity to take into account the effect was performed comparing the obtained torques with the rated ones for the motors. The parameters of the Γ -shaped equivalent scheme $R'_1, X'_1, R''_2, X''_2, X_\mu$ are shown in handbook [32] and given in relative units (r.u.).

The obtained dependences $M_{start}/M_N = f(P_2)$ for indicated motors are presented in Fig.1.1., where P_2 is motor rated power. If starting torque value calculated in such a manner is greater than the nominal one, here it is accepted that the impact of skin effect will be small and such motors should not be subjected to research.

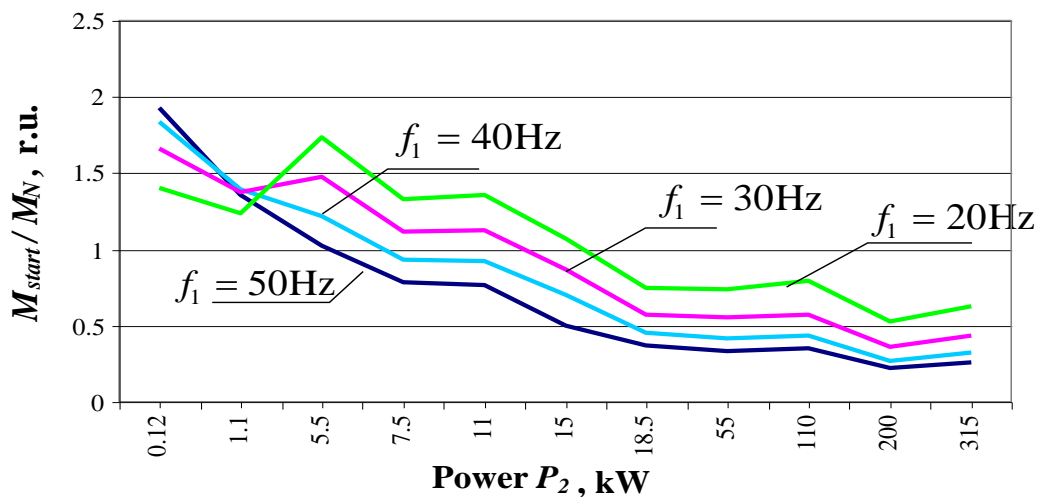


Fig.1.1. Calculated dependence of M_{start}/M_N on the motor rated power P_2 value at different frequencies f_1 of supply voltage for rated power range of motors A4 from 0.12 kW to 315 kW, if the parameters correspond to the nominal one.

Based on the the obtained correlations (Fig. 1.1), the following conclusions can be drawn for considered *A4* squirrel-cage induction motors with $p = 2$ in the power range 0.12 – 315 kW. The current displacement effect has to be taken into account only for **high power** SCIM (at 50 Hz over 10 kW). For **low power** SCIM this appearance can be ignored. If **high power** motor operating frequency is less than 50 Hz, the range of research is lower, which indicates that at the frequency tuning the rotor parameters changes are not significant.

1.2. Rotor Parameter Determination Using Fild's Coefficients

According to A. Fild [2] and F. Emde [1], the resistance of a rectangular rod is calculated by a conditional depth of current penetration h_r , while the inductance — by depth h_x :

$$h_r = \frac{h_{stien}}{\varphi(\xi)}, \quad h_x = h_{stien} f(\xi), \quad (1.1)$$

where h_{stien} is the total height of the conductor.

In the calculations, it was found convenient to define not just the rod resistance and inductance with uneven current density but also their relative changes under the effect of current displacement. These changes are estimated with Fild's coefficients k_r and k_x .

Analytical equations for defining k_r and k_x (obtained for rectangular bars under the assumption of the material resistivity constancy over the entire area of its cross-section, the infinity of the magnetic permeability of steel, and the straightness of magnetic flux linkage lines in the slot) are:

$$k_r = \xi \cdot \frac{sh2\xi + \sin 2\xi}{ch2\xi - \cos 2\xi} = \varphi(\xi) \quad (1.2)$$

$$k_x = \frac{3}{2\xi} \cdot \frac{sh2\xi - \sin 2\xi}{ch2\xi - \cos 2\xi} = f(\xi)$$

In these equations, ξ is the so-called reduced height of the bar rod — i.e. a dimensionless quantity, the value of which is determined by the equation:

$$\xi = 2\pi h_{stien} \sqrt{\frac{f_2}{\rho} \cdot \frac{b_{stien}}{b} \cdot 10^{-7}}; \quad (1.3)$$

where b_{stien} and b are the width of the rod and the slot, respectively (since the rotor winding is usually not insulated, $b_{stien} = b$);

f_2 is the frequency of current in the rotor;

ρ is the resistivity of the rotor rod material at the estimated temperature.

The phase resistance of squirrel-cage rotor windings with a current displacement can be calculated as (6-164) [30]:

$$R_2 = k_r R_{stien} + \frac{2R_{gr}}{\Delta^2}, \quad (1.4)$$

where R_{stien} is slot zone resistance of rod winding;

R_{gr} is closed ring zone resistance;

Δ is transformation coefficient of closed ring current to the rod current (6-72) [30]:

$$\Delta = 2 \sin \frac{\pi p}{Z_2} \quad (1.5)$$

The phase inductance of squirrel-cage rotor windings with a current displacement (CD) can be calculated as follows (6-173) [30]:

$$X_{\sigma 2} = 7.9 \cdot 10^{-6} f_l l_{\delta} (k_x \lambda'_{stien} + \lambda_f + \lambda_d), \quad (1.6)$$

where λ'_{stien} is magnetic conductivity coefficient of rod at tab. 6-23 [30];

λ_f is magnetic conductivity coefficient of frontal dissipation as (6-176) [30];

λ_d is magnetic conductivity coefficient of differential dissipation as (6-174) [30];

f_l is the frequency of supply voltage;

l_{δ} is an air gap length.

1.3. Rotor Parameter Determination Based on a Multi-Link Circuit

The author has accepted the same approach as in [30], i. e. the equivalent scheme of a rotor with variable parameters influenced by the current displacement effect could be presented as a multi-link circuit with constant and current displacement independent impedances (Fig. 1.2).

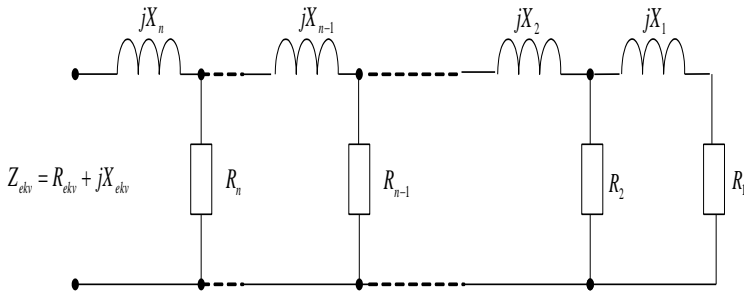


Fig 1.2. The multi-link circuit of rotor rod.

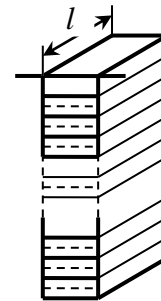


Fig. 1.3. Division of a solid rod into elementary layers.

Then, the author proposed the method for calculation of the rotor rod with a displacement of the electric current density in the multi-link scheme of impedances that is based on the following assumptions.

Knowing the magnetic line configuration of the flux linkage in a rotor slot, we can divide a massive electrical conductor (a squirrel-cage winding solid rotor rod) into a number of elementary layers separated from each other by thin insulation layers (Fig. 1.3). We will assume that there is a plane-parallel field in the slot and that the electric current density along the line of flux is constant. Since the height of an elementary layer is comparatively small, these allowances do not introduce any considerable errors into the calculations.

Therefore, the parameters of equivalent scheme (see Fig. 1.2) are resistance R_i and inductance X_i of the i -th elementary layer:

$$R_i = \rho l / q_i \quad (1.7)$$

where ρ is the resistivity of the rotor rod material at temperature of calculation;

$q_i = h_i b_i$ is the cross-sectional area of the i -th layer;

b_i is the average width of the i -th layer;

$h_i = h_{pos} / n_{pos}$ is the average height of the i -th layer;

n_{pos} is a number of elemental layers in slot;

l is the length of the i -th elementary layer;

and

$$X_i = \omega_2 \mu_0 \lambda_i l = 2\pi f_1 s \mu_0 \lambda_i l \quad (1.8)$$

where ω_2 is the angular frequency of the rotor bar current;

$\lambda_i = h_i / b_i$ is the conductivity of a geometrical magnet tube whose boundaries are defined by the i -th elementary layer;

μ_0 —magnetic constant, $\mu_0 = 4\pi \cdot 10^{-7}$ H/m.

Thereby determining the rotor equivalent impedance Z_{ekv} , the results are the rotor rod resistance $R_{ekv} = R_{stien}$ and inductance $X_{ekv} = X_{stien}$.

1.4. Rotor Parameters Determination Using the Software System

QuickField 5.7

One of the ways to give the rotor parameters is multifunctional software system *QuickField 5.7*, which is based on the method of finite elements for the calculation

(mathematical modelation) of the magnetic fields. In the present research, the problem of plane parallel field in section «The magnetic field of alternating currents» is solved.

The topological model for a given slot was created in *QuickField 5.7* environment.

Creation of the model occurs in three stages:

1. The topological model of calculated area designing and description — setting the vertices and edges, which covers the blocks with different physical parameters (environmental material properties, field sources), the result is placed in data base as file type ***mod*.

2. Setting the material properties, field sources and boundary conditions, giving for identifiers these elements. This task parameters are placed in data base as file type ***dhe*.

The following material properties (**bloc identifiers**) are set in all the models:

- the magnetic permeability of air gap (two components of the plane parallel field) $\mu_x = 1$ and $\mu_y = 1$;
- the magnetic permeability of rotor core steel $\mu = 1000$;
- core material of squirrel cage — aluminum with the magnetic permeability (two components of the plane parallel field) $\mu_x = 1$ and $\mu_y = 1$ and conductivity $g = 20.5 \cdot 10^6$ S/m.

The core of the rotor is the source of the field in all the models. In the massive conductor the total current is given, and the current value is taken arbitrarily that does not affect the determined parameters (resistance and inductance).

The parameters of topological model **edge identifier** are the first type of boundary conditions. The first type or Dirihle boundary condition at the border is the known vector potential numerical value $A_0 = 0$.

3. Creating of the finite element mesh. A finite element mesh was built in automatical regime. It is possible to build a very dense mesh in some areas and sparse in others, because a method of geometrical decomposition ensures a smooth transition from small to larger items.

In the solving process of the *QuickField 5.7* task one more file is created, which is written as a result of the calculation — file type ***res*.

1.5. Rotor Parameter Determination Using Catalog Data

This section describes the author's proposed method that allows determining the slip-dependent rotor parameters using SCIM catalog data [32]. The following data can be considered: the stator resistance and inductance R_I and X_I , as well as the torque values M_i , which correspond to certain fixed slip values s_i . Nominal slip value s_N corresponds the nominal torque M_N , critical

slip s_{kr} — to the maximum torque M_{max} , slip value $s = 0.8$ — to the minimum torque M_{min} (in certain cases the minimum torque can be defined by a different slip value in the range $0.7 \leq s \leq 0.9$), slip value $s = 1$ — starting torque M_{start} (Fig. 1.4).

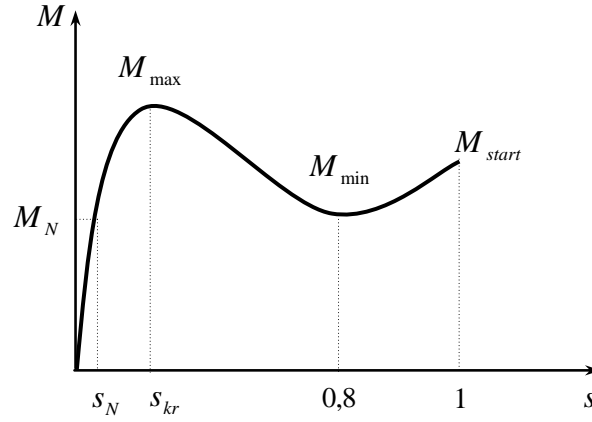


Fig.1.4. The squirrel-cage induction motor torque dependence on the slip.

Determining the rotor parameters, the known [19] induction motor electromagnetic torque equation (1.9) is accepted as a basis

$$M = \frac{pm_i}{\omega_1} \frac{U_1^2 \frac{R_2'}{s}}{\left(R_1 + c_1 \frac{R_2'}{s}\right)^2 + (X_1 + c_1 X_2')^2} \quad (1.9)$$

which is used in a transformed form:

$$m = \frac{M}{M_N} = \frac{R_{2e}/s}{(R_1 + R_{2e}/s)^2 + (X_1 + X_{2e})^2}. \quad (1.10)$$

Whereas the catalog provides the information about the curve $M = f(s)$ (Fig.1.4) expressed points, the rotor parameters R_{2e} and X_{2e} should set a greater number of points. Then the dependence $M = f(s)$ would need to be approximated by a mathematical equation:

- in range $0 < s \leq s_{kr}$ with a third-degree polynomial

$$m = a_3 s^3 + a_2 s^2 + a_1 s, \quad (1.11)$$

- in range $s_{kr} \leq s \leq s_l$ with a fourth-degree polynomial

$$m = b_4 s^4 + b_3 s^3 + b_2 s^2 + b_1 s + b_0. \quad (1.12)$$

Polynomial (1.10) and (1.11) coefficients can be found in the catalog, using the information on the torque M_i in typical slip points s_i . In order to determine three coefficients a_3 , a_2 , a_1 in equation (1.11) and five coefficients b_4 , b_3 , b_2 , b_1 , b_0 in equation (1.12) the three and five equations are required respectively. Therefore, the derivatives of the given expressions should be used:

$$\frac{dm}{ds} = 3a_3s^2 + 2a_2s + a_1 \quad (0 < s \leq s_{kr}), \quad (1.13)$$

$$\frac{dm}{ds} = 4b_4s^3 + 3b_3s^2 + 2b_2s + b_1. \quad (s_{kr} \leq s \leq s_l), \quad (1.14)$$

In addition it should be noted that in points $s = s_{kr}$ and $s = 0.8$ $dm/ds = 0$.

Expressing from (1.10) inductance X_{2e} , we obtain

$$X_{2e} = \sqrt{\frac{1}{m} \frac{R_{2e}}{s} - \left(R_1 + \frac{R_{2e}}{s}\right)^2} - X_1 \quad (1.15)$$

After reduction we obtain

$$\frac{dm}{ds} = \frac{4m \left(R_1 + \frac{R_{2e}}{s}\right) \left(\frac{dR_{2e}}{ds} s - R_{2e}\right)}{s^2 \left(1 - m \frac{R_{2e}}{s}\right)}. \quad (1.16)$$

In the beginning, the derivative dR_{2e}/ds is determined from the equation (1.16):

$$\frac{dR_{2e}}{ds} = \frac{\frac{dm}{ds} \frac{s}{4m} \left(1 - m \frac{R_{2e}}{s}\right)}{R_1 + \frac{R_{2e}}{s}} + \frac{R_{2e}}{s}. \quad (1.17)$$

Solving (1.17), the Euler's method can be used. According to this method, the resistance value corresponds to any slip s_i value and can be determined as

$$R_{2e,i} = R_{2e,i-1} + \Delta R_{2e,i} \quad (1.18)$$

where

$$\Delta R_{2e,i} = \left(\frac{dR_{2e}}{ds}\right)_{i-1} (s_i - s_{i-1}). \quad (1.19)$$

In addition, in equation (1.19) value $(dR_{2e}/ds)_{i-1}$ is determined from the right-hand side of equation (1.17), by inserting values $(dm/ds)_{i-1}$, M_{i-1} , R_{2e} and s_{i-1} obtained in the previous step i .

Let's review the solving algorithm, which is based on the following calculations. The current displacement effect in the rotor slots is not actually observed at a low slip value, the resistance is constant and, therefore, in equation (1.17) $dR_{2e}/ds = 0$ may be accepted. For accepted slip value m_0 can be calculated in (1.11), $(dm/ds)_{s=s_0}$ — in (1.13).

Then, equation (1.17) is converted into an algebraic equation and its solution gives $R_{2e,0}$, which corresponds to initial slip $s_{i-1} = s_0$ (it is desirable that $s_0 \leq 0.01$). Subsequently, the equivalent inductance $X_{2e,0}$ and electromagnetic torque $M_0 = m_0 \cdot M_N$, which corresponds to s_0 , have been calculated, using (1.15) and (1.10) respectively.

The whole slip change range $[s_0;1.0]$ is divided into k equal parts with step $h = (1.0 - s_0)/k$, as a result the argument has been obtained $s_i = s_0 + ih$ ($i = 0, 1, 2, \dots, k$). Then the next slip value is calculated as follows $s_I = s_0 + Ih$.

It is necessary to look for parameters corresponding to s_I : m_I — at (1.11) or at (1.12), $(dm/ds)_{s=s_I}$ — in (1.13) or in (1.14). Using (1.19), define the corresponding $\Delta R_{2e,I}$, rotor equivalent resistance $R_{2e,I}$ — at (1.18), equivalent inductance $X_{2e,I}$ at (1.15), $M_I = m_I M_N$ — at (1.10). The calculation is repeated.

Review of methods indicates that many options are available to solve the formulated tasks by various methods (using different methods). The formulated methods show that it is necessary to take into account the rotor slot form. The author's proposed calculation methods of parameters during the transient processes with multi-link circuit and using catalog data are a good alternative to other authors' suggested solutions. The accuracy of the author's proposed methods is required for the comprehensive examination.

2. THE CALCULATIONS OF THE ROTOR VARIABLE PARAMETERS WITH DIFFERENT METHODS

In this chapter, based on the methods proposed in Chapter 1, the calculations of variable rotor parameters are carried out for chosen *A4* series high power *4AH355S4V3* 315 kW and low power *4A90L2V3* 3 kW squirrel-cage induction motors with various slot configurations. The comparative analysis of the calculation results is shown, the application possibility of different methods and their calculation accuracy are evaluated.

The topological models of slot and the magnetic field distribution for chosen motors at the different frequencies with software system *Quick Field 5.7* are created (Fig. 2.1 and Fig. 2.2).

Obtained field scenes (Fig. 2.1) of **high power** SCIM testify that at slip s values close to singleton, the magnetic flux lines are concentrated in the upper part of the slot. Accordingly, the current density of these slot layers is higher. At the small slip s values the magnetic flux lines and, at the same time, the current density is evenly distributed over the height of the slot.

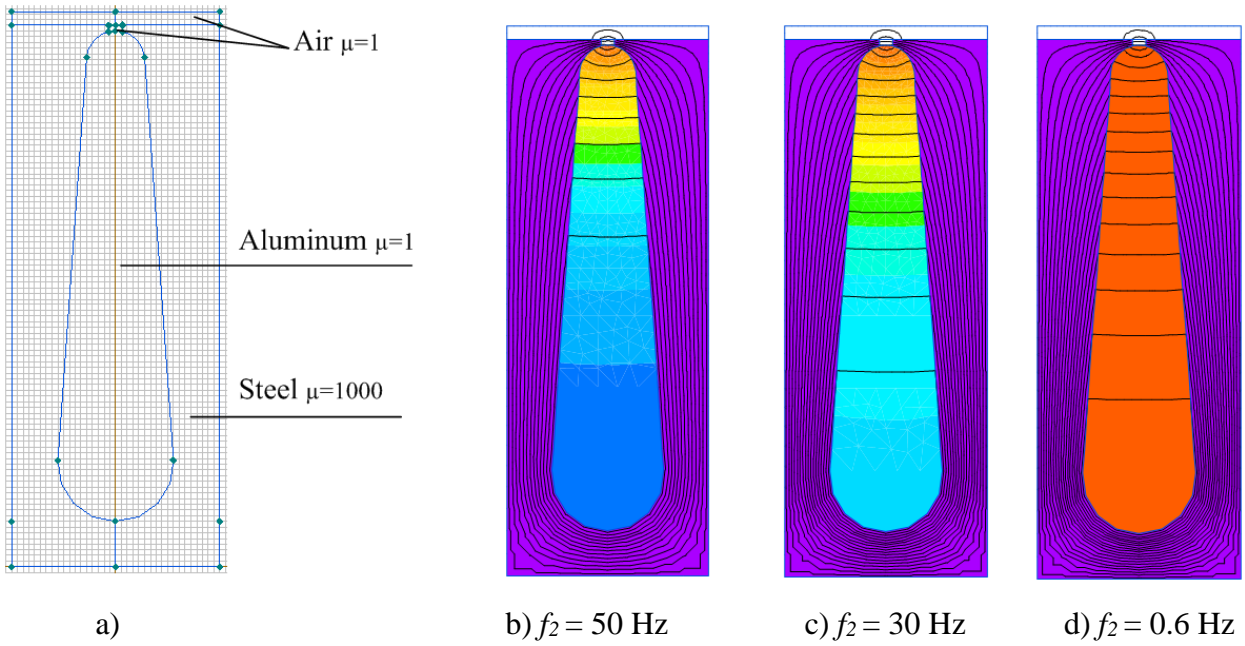


Fig. 2.1. The topological model (a); field distribution in the slot at different frequencies b) – d) for SCIM 4AH355S4V3 315 kW.

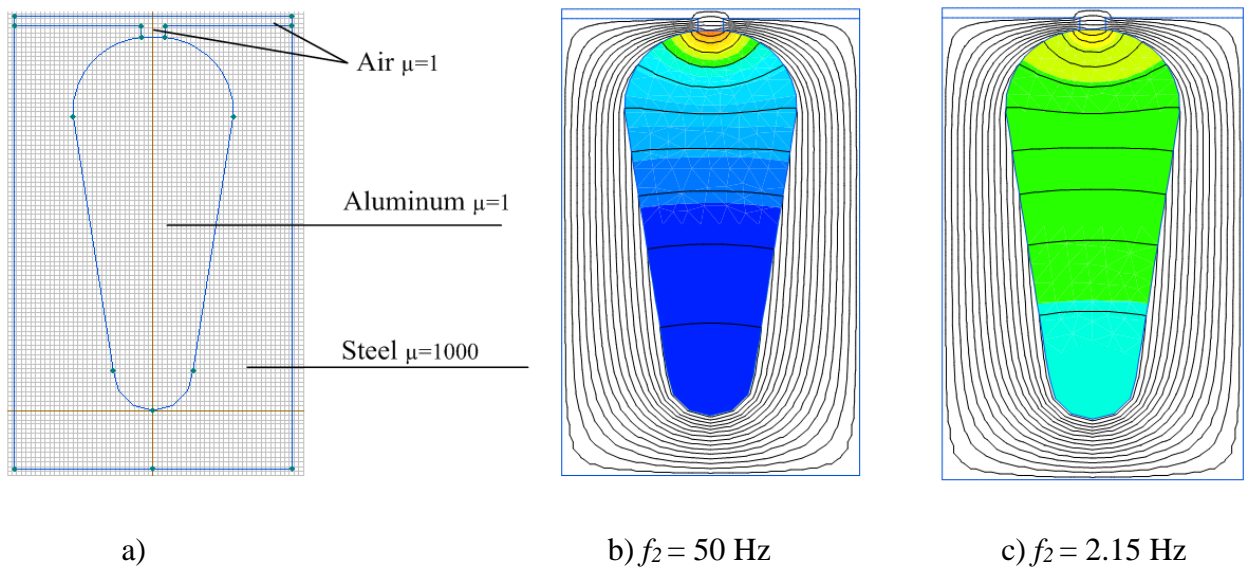


Fig. 2.2. The topological model (a); field distribution in the slot at different frequencies b) – c) for SCIM 4A90L2V3 3 kW.

For **low power** 4A90L2V3 3 kW SCIM (Fig. 2.2) the magnetic flux lines are practically evenly distributed over the height of the slot. It allows concluding that the distribution of magnetic flux during the start-up is not dependent on the current displacement effect.

The resistance and inductance for the chosen SCIM have been calculated with different methods. The graphic dependences $R'_2 = f(s)$ and $X'_2 = f(s)$ in r.u. for the SCIM 4AH355S4V3 315 kW are presented in Fig. 2.3.

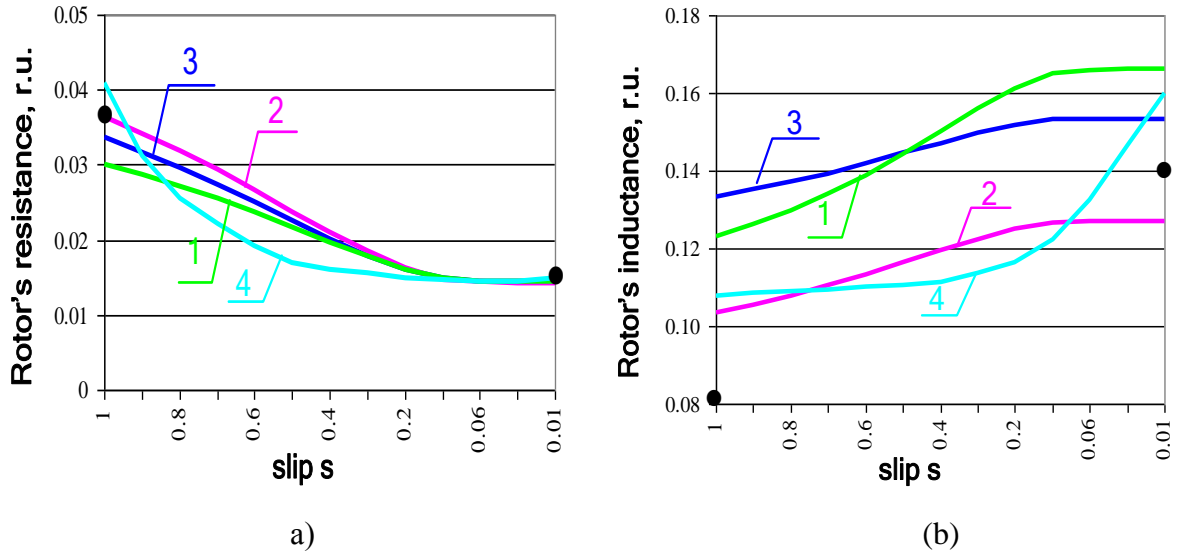


Fig. 2.3. SCIM 4AH355S4V3 315 kW rotor start-up resistance (a) and inductance (b):
 1 — obtained using Fild’s coefficients; 2 — obtained using the multi-link circuit;
 3 — obtained using *Quick Field*; 4 — obtained using catalog data.

From the obtained dependence (Fig. 2.3. a) it is obvious that during the start-up moment at $f_2 = 50$ Hz ($s = 1$) the rotor resistance reaches its maximum value. With the acceleration of the motor, the slip reduces as well as the value of the rotor resistance reduces, reaching its nominal value.

The comparison of SCIM 4AH355S4V3 315 kW resistances, obtained by different methods, with catalog data are presented in Table 2.1 (in r.u.). The most accurate results are provided by the method, which is based on the rotor slot equivalent multi-link circuit. The least accurate results have been obtained, using method with Fild’s coefficients.

Table 2.1

The Comparison of SCIM 4AH355S4V3 315 kW Resistances, Obtained by Different Methods, with Catalog Data

Parameters	Mode of operation			
	start-up	variation %	nominal	variation %
Catalog data	0.038		0.014	
Using Fild’s coefficients	0.03	21.05	0.01437	2.64
Using the multi-link circuit	0.03613004	4.92	0.0143268	2.33
Using <i>QuickField 5.7</i>	0.0337	11.3	0.01442	3
Calculation, using catalog data	0.041	7.89	0.015	7.14

From the obtained dependences (Fig. 2.3. b), it is obvious that during the start-up process at $f_2 = 50$ Hz ($s = 1$) the rotor inductance reaches its minimum value. With the acceleration of the motor, the slip reduces whereas the value of the inductance increases.

The comparison of SCIM 4AH355S4V3 315 kW inductances, obtained by different methods, with catalog data is presented in Table 2.2 (in r.u.). The most accurate results are provided by the method, which is based on the rotor slot equivalent multi-link circuit.

Table 2.2

The Comparison of SCIM 4AH355S4V3 315 kW Inductances, Obtained by Different Methods, with Catalog Data

Parameters	Mode of operation			
	start-up	variation %	nominal	variation %
Catalog data	0.08		0.14	
Using Fild's coefficients	0.1231	53.87	0.166367	18.83
Using the multi-link circuit	0.103647	29.55	0.127417	8.9
Using <i>QuickField 5.7</i>	0.1334	65.75	0.154	10
Calculation, using catalog data	0.108	35	0.16	14.29

The comparison of resistance and inductance obtained by different methods for SCIM 4A90L2V3 3 kW is presented in Fig. 2.4.

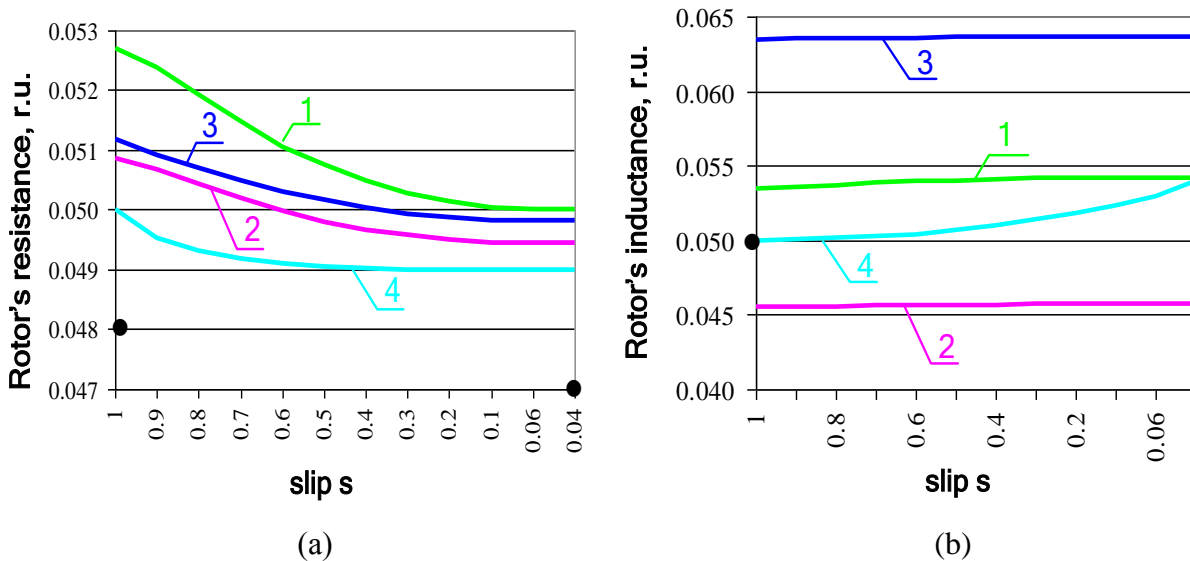


Fig. 2.4. SCIM 4A90L2V3 3 kW rotor start-up resistance (a) and inductance (b):
 1 — obtained using Fild's coefficients; 2 — obtained using the multi-link circuit;
 3 — obtained using *Quick Field*; 4 — obtained using catalog data.

From the obtained dependence (Fig. 2.4. a) it is obvious that during the start-up moment at $f_2 = 50$ Hz ($s = 1$) the rotor resistance reaches its maximum value. With the acceleration of the motor, the slip reduces as well as the value of the rotor resistance **negligibly** reduces, reaching its nominal value.

From the obtained dependences (Fig. 2.4. b) it is obvious that during the start-up process at $f_2 = 50$ Hz ($s = 1$) the rotor inductance reaches its minimum value. With the acceleration of the motor, the slip reduces whereas the value of the inductance **negligibly** increases.

The comparison of SCIM 4A90L2V3 3 kW resistances, obtained by different methods, with catalog data is presented in Table 2.3 (in r.u.). All methods, which have been used for calculations of rotor parameters, give the results with almost the same accuracy.

Table 2.3

The Comparison of SCIM 4A90L2V3 3 kW Resistances, Obtained by Different Methods, with Catalog Data

Parameters	Mode of operation			
	start-up	variation %	nominal	variation %
Rotor resistance, r.u.				
Catalog data	0.048		0.047	
Using Fild's coefficients	0.0527	9.79	0.0501	6.59
Using the multi-link circuit	0.050872	5.98	0.04955	5.42
Using <i>QuickField 5.7</i>	0.05119	6.65	0.04982	6
Calculation, using catalog data	0.05	4.17	0.049	4.26

The comparison of SCIM 4A90L2V3 3 kW inductances, obtained by different methods, with catalog data is presented in Table 2.4 (in r.u.). The most accurate results are provided by the method using Fild's coefficients.

The results of rotor resistance and inductance calculations allow accepting that, having calculated the variable rotor parameters, the current displacement effect in rotor slots is taken into account for **high power** motors. This phenomenon can be ignored for **low power** motors. The author's proposed method for calculation of the rotor parameters, based on the slot **multi-link circuit**, provides the high-precision of calculations. This method can be used not only for calculations (or specifying) the rotor parameters of existing motors, but also in **designing of new SCIM with arbitrary rotor slot configuration**.

Table 2.4

The Comparison of SCIM 4A90L2Y3 3 kW Inductances, Obtained by Different Methods, with Catalog Data

Parameters	Mode of operation			
	start-up	variation %	nominal	variation %
Rotor inductance, r.u.				
Catalog data	0.053		0.1	
Using Fild's coefficients	0.053527	0.99	0.054231	
Using the multi-link circuit	0.04551	14.10	0.04578	
Using <i>QuickField 5.7</i>	0.06348	19.77	0.06368	
Calculation, using catalog data	0.05	5.66	0.054	

3. MATHEMATICAL MODELS OF A SQUIRREL-CAGE INDUCTION MOTOR AND THEIR APPLICATION IN THE RESEARCH OF TRANSION PROCESS WITH ROTOR CURRENT DISPLACEMENT EFFECT

This chapter is devoted to the calculations of the SCIM transion process taking into account the rotor variable parameters; to the review of accepted mathematical models; to the choice of coordinate system and basic parameters.

Phenomena that accompany the transion process in electrical motors are extremely difficult. Creating mathematical correlations and regularities, which are wholly subordinate to the transion process flowing, is practically impossible due to great mathematical difficulties and complicating formulas [49].

Therefore, in mathematical modelling it is necessary to take into account only the main factors, neglecting the minor edicts [16], [31]. For this purpose, the idealized SCIM is reviewed. For this idealized SCIM the magnetic circuit is not saturated, the hysteresis phenomenon and the loss in steel (Fuko current) have not been considered, the magnetomotive force (m. s.) and the induction distribution in space have been adopted (accepted) sinusoidal (higher harmonics is not taken into account), leakage inductances are accepted regardless of the rotor position. For the purpose of simplicity, it is generally believed, that parameters do not depend on SCIM currents and rotation speed, as well as the resistances — on temperature.

The induction motor (IM), whose stator and rotor windings are three-phase, the rotor windings are considered to have been reduced to stator windings, winding connection is “star / star”, three-phase IM windings are moved at angle 120 el. deg., the air gap is even, rotor is symmetrical, the stator windings are symmetrical, is considered in mathematical modelling [27], [31], [49].

IM voltage equation will be written considering the energy direction from the network to the shaft positive. This corresponds to IM motor operating mode.

The relative units (r.u.) have been accepted to be used in the present research for transient process calculations, as well as the base values of the stator and rotor circuit have been formulated.

The IM nonlinear differential equation system in phase coordinates with periodic coefficients has been created in the present research. To obtain the system of equations with constant coefficients, the coordinate transformation along two perpendicular axes has been carried out. As a result, IM model has been obtained in $d, q, 0$ coordinates, the axis of which is fixed in relation to rotor and rotates in relation to stator with rotor rotation speed, i.e. $\omega_k = \omega_r = \omega$. This coordinate transformation allows using IM model for the calculations of transient process with variable rotor parameters [35], [38]. The IM $d, q, 0$ coordinate system is presented in Fig. 3.1.

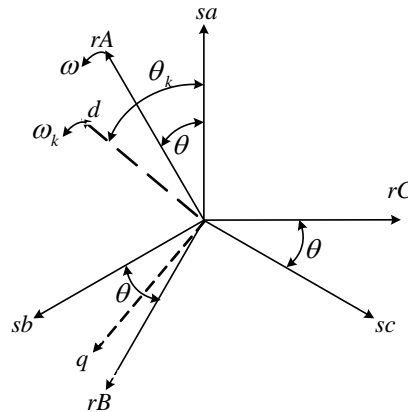


Fig. 3.1. The induction motor $d, q, 0$ coordinate system.

The simplest algorithm, which is written in a matrix form and allows using the standard procedures of integration, is used for IM transient process calculations.

Equations (3.1) and (3.3) [27] to be resolved for the calculation of the transition process of IM

$$\frac{d}{d\tau}[I] = [A]^{-1} \cdot [D], \quad (3.1)$$

where matrices are

$$[A] = \begin{bmatrix} X_s & 0 & X_{ad} & 0 \\ 0 & X_s & 0 & X_{ad} \\ X_{ad} & 0 & X_r & 0 \\ 0 & X_{ad} & 0 & X_r \end{bmatrix}; \quad [I] = \begin{bmatrix} i_{sd} \\ i_{sq} \\ i_{rd} \\ i_{rq} \end{bmatrix};$$

$$[\Psi] = \begin{bmatrix} \Psi_{sd} \\ \Psi_{sq} \\ \Psi_{rd} \\ \Psi_{rq} \end{bmatrix}; \quad [D] = \begin{bmatrix} u_{sd} - R_s i_{sd} + \omega_k \Psi_{sq} \\ u_{sq} - R_s i_{sq} - \omega_k \Psi_{sd} \\ -R_r i_{rd} + (\omega_k - \omega) \Psi_{rq} \\ -R_r i_{rq} - (\omega_k - \omega) \Psi_{rd} \end{bmatrix}. \quad (3.2)$$

$$\frac{d\omega}{d\tau} = [X_{ad}(i_{rd}i_{sq} - i_{rq}i_{sd}) - M_{sl}] / T_M, \quad (3.3)$$

where M_{sl} — the load torque, which determined the drive;

T_M — the inertial constant of IM and drive in synchronous seconds.

The rotor variable **inductance** X_r is included in matrix $[A]$, the rotor variable **resistance** R_r — in matrix $[D]$.

The calculations performed in the second chapter made it possible to find the most convenient and accurate method for the calculations of rotor parameters in matrices $[A]$ and $[D]$. It is the author's own developed method, based on the multi-link circuit, which will be used hereafter for the calculations of referred matrices of rotor parameters during the IM transient process, i. e. to solve equations (3.1).

The author has created a block scheme and software for calculations of IM transient process with variable rotor parameters.

4. THE CALCULATIONS OF THE TRANSIENT PROCESS OF INDUCTION MOTOR WITH ROTOR VARIABLE PARAMETERS

4.1. The Calculation Using the Software Created by the Author

This chapter is dedicated to research of transient process for the chosen induction motor.

The rotor resistance and inductance calculation results (the second chapter) allow accepting that the calculated variable rotor parameters, the current displacement effect have to be taken into account only for **high power** motors. This phenomenon can be ignored for **low power** motors.

Therefore, the calculation of the transition process is carried out for the subsequent 4A series 4AH355S4Y3 315 kW type of motor. The equations for the calculation of IM transition process in the relative units (r.u.) have been made in the third chapter. The rotor resistance and

inductance in the aforementioned equations are variable parameters. The calculation of IM transient process is carried out, using the method of rotor parameter calculations set out in the first chapter.

The author has developed software for calculations of SCIM transient process with variable rotor parameters for the chosen motor. The following parameters have been chosen as the basic data for calculations:

U_l and I_l are stator phase voltage [V] and current [A];

f_l is supplying source frequency [Hz];

R_l is stator winding resistance r.u.;

X_l is stator winding inductance r.u.;

$X_\mu = X_{ad}$ is the inductance of magnetisation circuit r.u.;

rotor slot form (configuration) and sizes [mm];

ρ is resistivity of rotor winding material [$\Omega \cdot \text{mm}^2/\text{m}$].

The load simulation (in r. u.) can be described as

$$M_{load} = M_c + k\omega^2 \quad (4.1)$$

where $M_c = 0$ is the static component of torque;

$k = 0.702$ is a load coefficient.

The torque of inertia J [$\text{kg} \cdot \text{m}^2$] is simulated with the mechanical time constant T_M :

$$T_M = \frac{Jn_N}{9.55M_N} \cdot 314.159 \quad (4.2)$$

For motor 4AH355S4V3 315 kW:

$$T_M = \frac{Jn_N}{9.55M_N} \cdot 314.159 = \frac{5.8 \cdot 1500}{9.55 \cdot 2032} \cdot 314.159 = 0.448 \cdot 314.159$$

The dynamic characteristics $I = f(t)$, $M_{em} = f(t)$, $n = f(t)$ have been obtained as a result of the transient process calculations.

The dynamic characteristics ($I = f(t)$, $M_{em} = f(t)$, $n = f(t)$) for high power SCIM 4AH355S4V3 315 kW for setting the resistance and inductance of rotor in different ways are presented in Fig. 4.1.

The dependence of start/nominal value ratio as well as the duration of the transient process from calculation ways of rotor variable parameters (the comparison with different method results) for SCIM 4AH355S4V3 315 kW is presented in Table 4.1.

The performed calculations show that rotor variable parameters **noticeably** impact the transion process of high power SCIM.

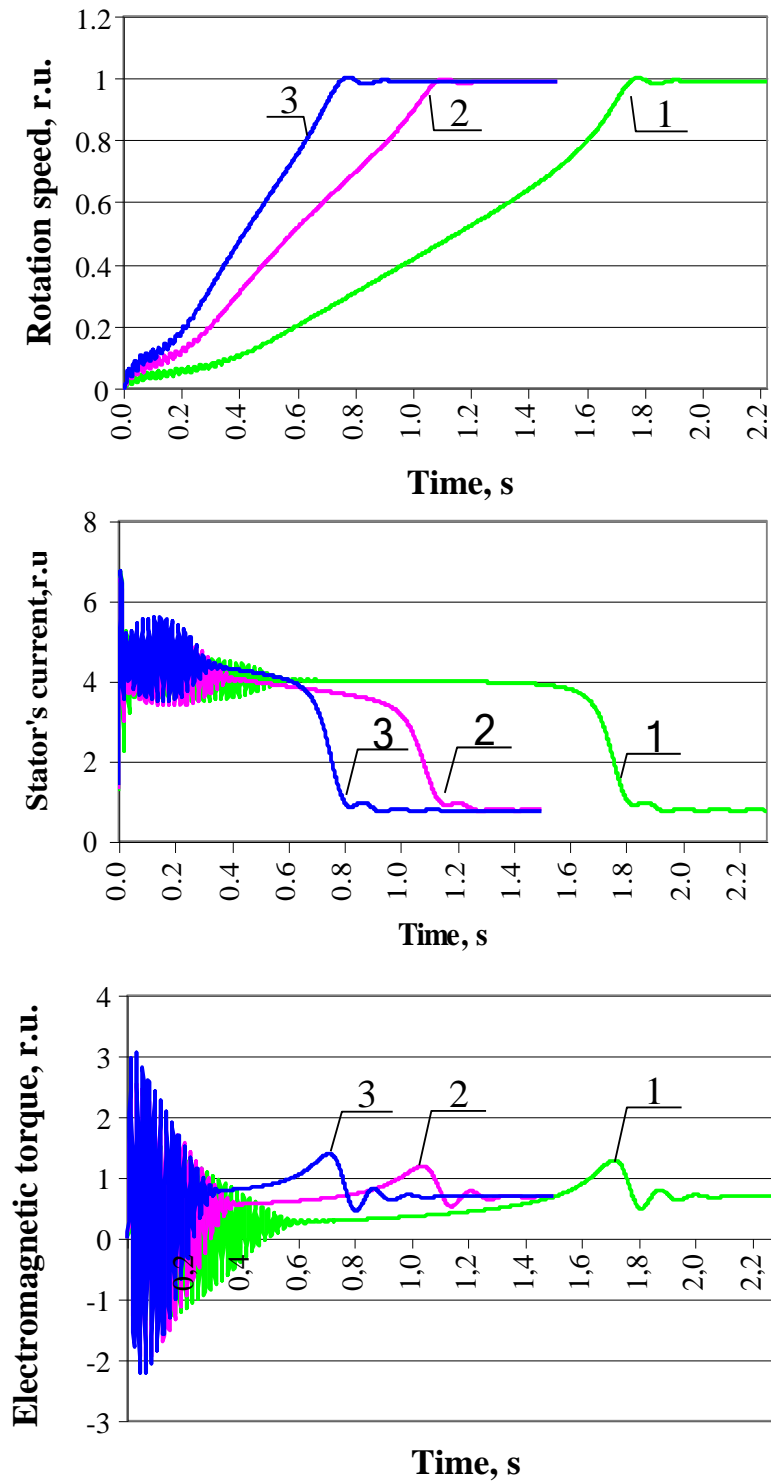


Fig. 4.1. Dynamic characteristics of SCIM 4AH355S4V3 315 kW for setting the parameters of rotor in different ways:

- 1 — mode of operation with constant rotor parameters $R_{2N}'' = 0.014$ r.u. and $X_{2N}'' = 0.14$ r.u. at nominal mode;
- 2 — mode of operation with variables at start-up rotor parameters R_2'' and X_2'' , using Fild's coefficients;
- 3 — mode of operation with variables at start-up rotor parameters R_2'' and X_2'' , using a multi-link circuit.

4.2. The calculation of the SCIM Transient Process by *PSIM* Software Complex

Simulation of start-up in settings of the rotor **constant (nominal) parameters** $R'_{2N} = 0.014$ r.u. and $X'_{2N} = 0.14$ r.u. [28] for SCIM *4AH355S4Y3* 315 kW is presented in Fig. 4.3 b. The parameters [32] used in simulation are presented in Fig. 4.3 a.

In *PSIM* software complex, the calculations are carried out in physical units. In the author's proposed program the calculations are carried out in relative units. To carry out the calculations at the same load, the coefficient $k = 0.702$, which was used by the author's program, should be reduced to *PSIM* software complex as follows:

$$k = \frac{0.702M_N}{\omega^2} = \frac{0.702 \cdot 2032}{155^2} = 0.059$$

$$U_l = 660V$$

$$f = 50Hz$$

$$R_1 = 22.42m\Omega$$

$$L_1 = 0.4134mH$$

$$R'_{2N} = 16.52m\Omega$$

$$L'_{2N} = 0.525mH$$

$$L_\mu = 17.29mH$$

$$2p = 4$$

$$J_{d.r.} = 5.8kgm^2$$

$$M_{sl} = k\omega^2 = 0.059\omega^2$$

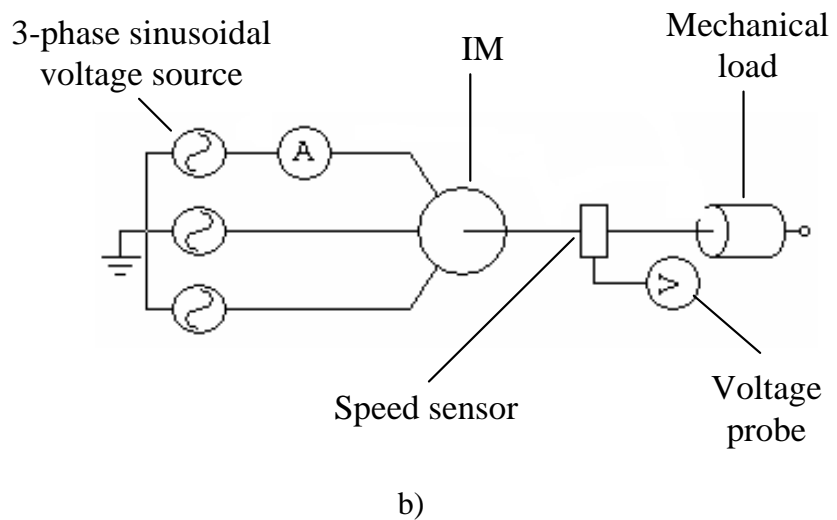


Fig. 4.2. Setting parameters a) and transient process modelation scheme with constant rotor parameters b) for SCIM *4AH355S4Y3* 315 kW.

The dynamic characteristics ($I = f(t)$, $M_{em} = f(t)$, $n = f(t)$) for high power SCIM *4AH355S4Y3* 315 kW are presented in Fig. 4.4 (a).

SCIM start-up simulation with program *PSIM* in settings of rotor **variable parameters** is based on the scheme that is presented in Fig. 4.2.

In each phase rotor circuit introduced five sections, which contain resistance (5.66 m Ω) and inductance (0.045 mH). SCIM start-up simulation with rotor **variable parameters** is presented in Fig. 4.3.

At start-up moment the nominal resistance 16.52 m Ω and starting inductance 0.3 mH are set. The rotor rotation speed control sensors are included in the rotor circuit. When SCIM

reaches certain rotation speed (150, 350, 600, 900, 1300 min⁻¹) the inductance is included in the rotor circuit, but resistance is replaced on short-circuit. Thereby, the decrease in resistance and the increase in inductance are simulated during SCIM start-up.

In order to verify the accuracy of calculations, a simulation scheme with 9 regulation sections was drawn up. But the obtained results suggest that the start-up (I_{pal} , M_{pal} , t_{pal}) and nominal (I_N , M_N) parameters are not dependent on the number of introduced sections. The simulation of SCIM transient process can make the scheme with 5 regulation sections.

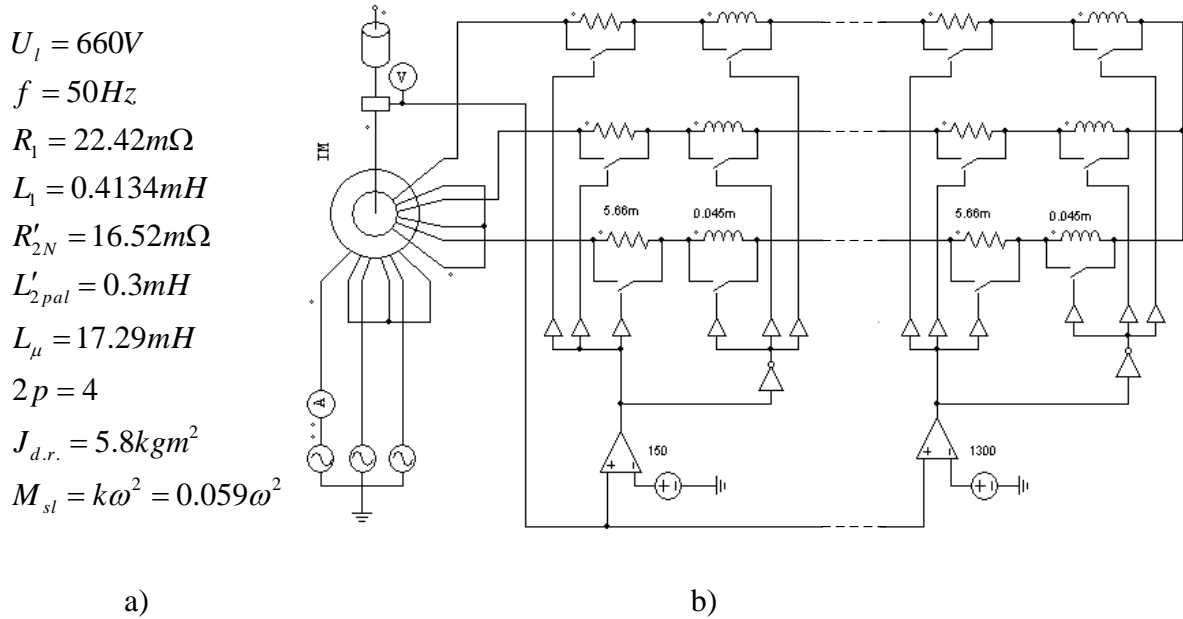


Fig. 4.3. Setting parameters a) and transient process simulation scheme with variable rotor parameters b) for SCIM 4AH355S4V3 315 kW.

Dynamic characteristics ($M_{em} = f(t)$, $n = f(t)$) of high power SCIM 4AH355S4V3 315 kW for setting the parameters of rotor (by the author's software (a) and by *PSIM* software complex (b)) in different ways are presented in Fig. 4.4.

According to *PSIM* software complex, the obtained simulation results well coincide with the computer calculation results by the author's proposed methods for the parameter change calculation. The dynamic characteristic of SCIM 4AH355S4V3 315 kW explicitly shows it (Fig. 4.4).

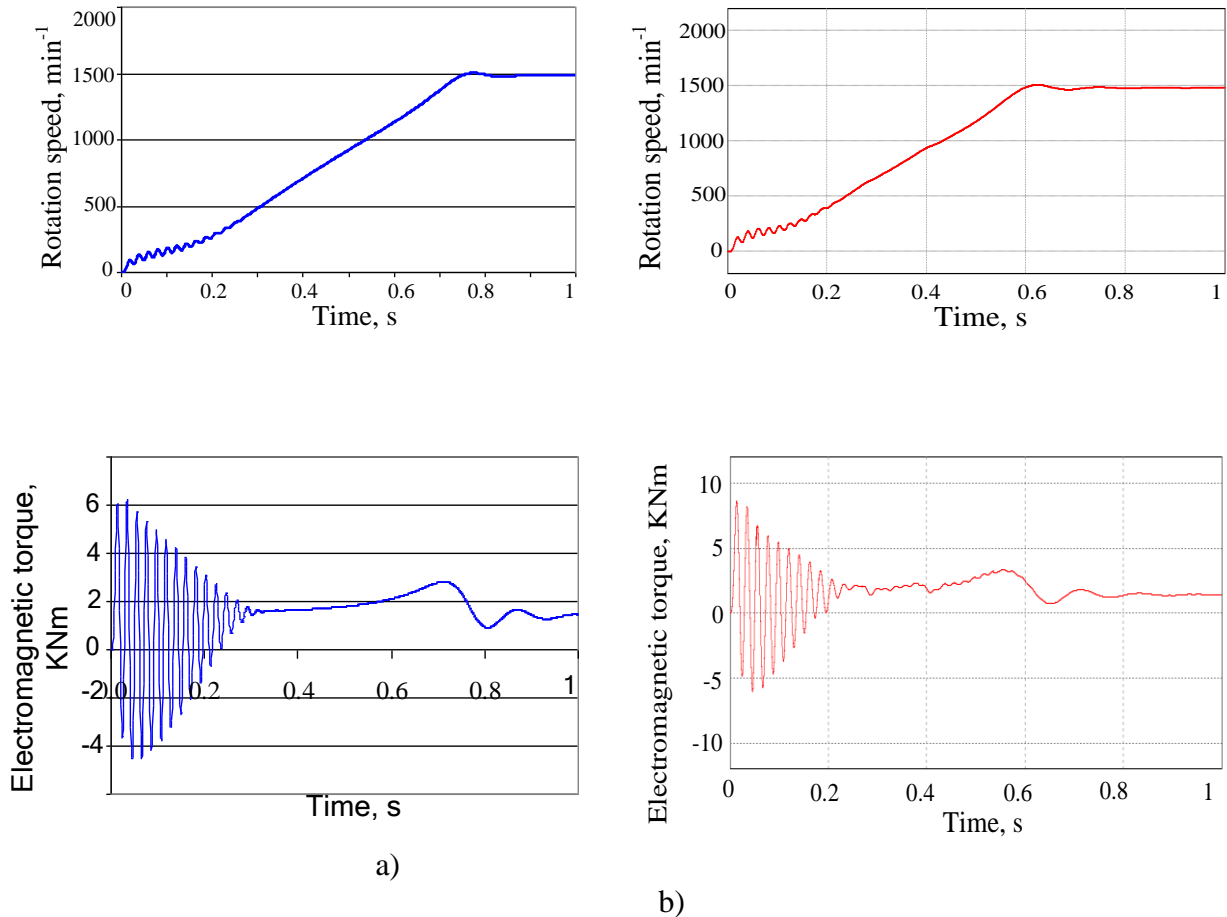


Fig. 4.4. Dynamic characteristics of SCIM 4AH355S4V3 315 kW for setting the parameters of rotor in different ways:

- a) — with variables at start-up rotor parameters, using the author's proposed program;
- b) — with variables at start-up rotor parameters, using *PSIM* software complex.

Dynamic characteristics of SCIM 4AH355S4V3 315 kW with constant (Fig. 4.2) and variable (Fig.4.3) rotor parameters are presented in Fig. 4.5.

The characteristics obtained by *PSIM* software complex (Fig.4.5) show, that the duration of transient process as well as the starting torque M_{start} and starting current I_{start} depend on the rotor variable parameters.

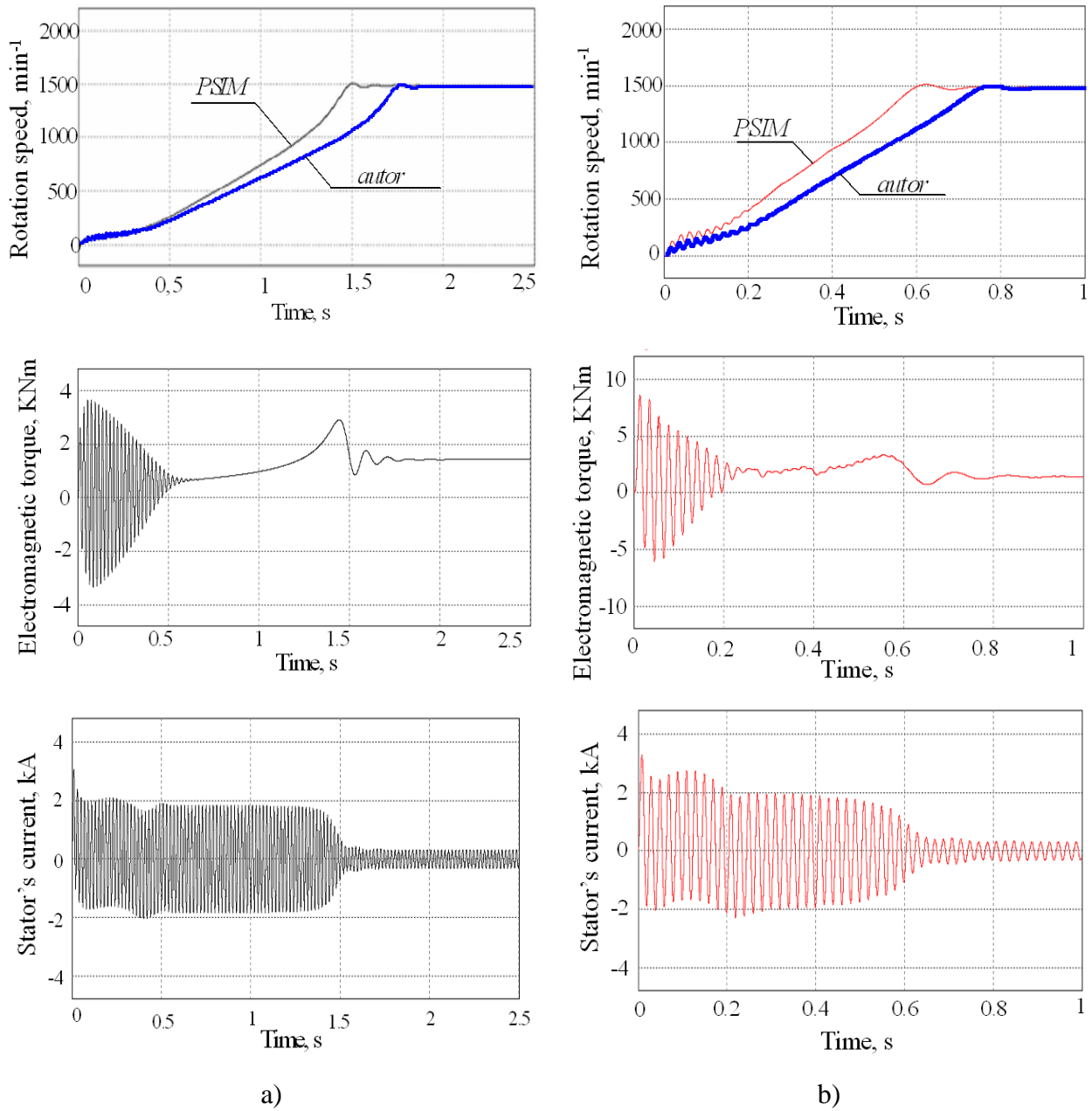


Fig. 4.5. Dynamic characteristics of SCIM 4AH355S4V3 315 kW, using *PSIM* software complex:
a) — with constant parameters at nominal mode;
b) — with variable parameters at start-up rotor parameters.

The comparison of starting parameters for SCIM 4AH355S4V3 315 kW at modes of operation with constant and variable rotor parameters is presented in Table 4.5.

Table 4.5

The Comparison of the Results Obtained by Various Methods

4AH355S4Y3 315 kW	Parameters	Starting torque ratio	Starting current ratio	Duration of start-up
		$\frac{M_{start}}{M_N}$	$\frac{I_{start}}{I_N}$	t_{start}, S
Using the author's program	With constant parameters	2.28	8.75	2.09
	Using Fild's coefficients	3.69	8.53	1.4
	Using multi-link circuit	4.45	8.77	0.85 – 0.9
Using <i>PSIM</i> software complex	With constant parameters	2.54	9.78	1.5 – 1.7
	With 5 regulation sections	6.02	9.93	0.85 – 0.9
	With 9 regulation sections	6.34	9.58	0.85 – 0.9

CONCLUSIONS

1. The results of rotor resistance and inductance calculations allow assuming that in calculation of the variable rotor parameters the current displacement effect in rotor slots must be taken into account only for **high power** motors (at 50 Hz above 10 kW). For **low power** motors this phenomenon can be disregarded. As the operating frequency of high power motor is less than 50 Hz and the research range at motor power is less, it indicates that the changes of rotor parameters are not significant at the frequency regulation.
2. The calculations of high power motor parameters, using Fild's coefficients, give relatively many errors in calculations of start-up regimes. This feature makes the use of this method undesirable.
3. Rotor parameter determination, using the software system *QuickField 5.7*, is cumbersome, because it requires the labor-intensive creation of topological model for slots with an arbitrary configuration and manual input of the rotor current frequency. This makes it impossible to use the calculated rotor parameters for simulation of SCIM transient process.
4. The author's proposed method for calculations of rotor parameters, **using a multi-link circuit**, gives relatively accurate results of calculations: the deviation of resistance value (relative error) from catalog data is 2.33–4.95 %; the deviation of inductance value — 8.9–29.55 %.
5. The author's proposed program, based on the **multi-link circuit**, makes it possible to **smoothly** change rotor parameters during the transient process. This makes the calculations of transition process corresponding to reality. This method can be used not only for rotor parameter calculations of existing motors, but also for designing of **new** SCIM with **arbitrary** rotor slot **configuration**.
6. The author's proposed method for calculations of rotor parameters, **based on the catalog data**, gives a satisfactory accuracy of calculations. However, this method can be used only for already designed motors, as well as for simulation of transient process of these SCIMs.
7. The simulation scheme of SCIM start-up with *PSIM* software complex in settings of rotor variable parameters has been created.
8. The performed calculations, using *PSIM* and the author's proposed program, have shown that for high power SCIM 315 kW the duration of transient process depends on the rotor parameters: with constant at nominal regime $t_{start} = 1.5\text{--}2.09$ s; with variable parameters

$t_{start} = 0.85\text{--}0.9$ s. The start/nominal torque ratio increases from values 2.54 r.u. to 6.34 r.u. by *PSIM* simulation results (2.28–4.45 r.u. by the author’s proposed program), the start/nominal current ratio almost does not depend on the calculation methods of the rotor parameters.

FUTURE RESEARCH

Within the framework of the Doctoral Thesis, the method for calculation of rotor parameters has been created, and direct start-up high power SCIM with loads of ventilator torque has been examined. The direct start-up is not a characteristic method in modern practice. Also, the load types may be different — compressor load, load with constant torque etc. In fact, the research should continue to investigate the frequently used dynamic modes for such motors as, for example, star–triangle start-up or motor start-up by “soft starting” method, when at constant stator voltage frequency motor starting current is limited, using the thyristor that smoothly changes the stator voltage. However, the research of such regimes requires long execution time and, therefore, could be the next author's subject of the research. It is also important to examine other real dynamic processes (reversing, braking, work with other loads), using the author’s proposed method for dynamic evaluation of rotor parameters. The author’s proposed method shows good opportunities of functional application.

LIST OF REFERENCES USED IN THE SUMMARY

1. Emde F. Einseitige Stromverdrängung in Ankernuten, E. und M., 1908, Bd. 24, p. 703–707.
2. Field A. B. Eddy currents in large slot-wound conductors, Trans AIEE, vol. 24, p. 761.
3. Ikeda M., Hiyama T. Simulation Studies of the Transients of Squirrel-cage Induction Motors//Energy Conversion, IEEE, 2007, № 22, p. 233–239.
4. Köhring P. Closed solution of the transient skin effect in induction machines// Electrical Engineering, 2009, № 91, p. 263–272.
5. Ku Y. H., Transient analysis of alternating current machinery, Trans. AIEE, 1929, v. 48, p. 707.
6. Levy W., Landy C. F. Уточненная модель для расчета глубокопазных асинхронных двигателей, Электротехника, 1991, № 8.
7. Li J., Xu L. Investigation of Cross-saturation and Deep Bar Effects of Induction Motors by Augmented dq Modeling Method//Industry Applications Conference, IEEE, 2001, p. 745-750.
8. Lin D., Zhou P. An Improved Dynamic Model for the Simulation of Three-phase Induction Motors with Deep Rotor Bars//Electrical Machines and Systems, ICEMS 2008. International Conference on, p. 3810–3814.
9. Liwschitz-Garik M. Calculation skin effect squirrel-cage rotors. Trans. AIEE T, 1955, v.74, III A, p. 768–771.
10. Lyon W. V., Transient analysis of alternating current machinery (book), 1954.
11. Meng D., Xia Y., Yang X. Dynamic Impedance Calculation for High-Voltage Motor in Starting Process// Industrial Engineering and Management Science, Pennsylvania, USA, 2013, p. 66–71.

12. Pedra J., Sainz L. Parameter estimation of squirrel-cage induction motors without torque measurements//IEE Electric Power Applications, 2006, vol. 153, № 2, p. 87–94.
13. Repo A.-K., et al. Dynamic Electromagnetic Torque Model and Parameter Estimation for a Deep-bar Induction Machine//IET Electric Power Applications, 2008, № 2, p. 183–192.
14. Verma C. P., Abo-Shady S. E. Method of calculation of transient skin-effect in conductors embedded in slot for cage winding, IEEE Trans. on PAS, 1981, № 6.
15. Wu X. Z., Wang X. H. Calculations of skin effect for double-cage rotor bar of the induction machine, CSEE, 2003, № 23(3), p. 116–119.
16. Важнов А. И. Переходные процессы в машинах переменного тока. Л.: Энергия, 1980, с. 256.
17. Веников В. А. Переходные электромеханические процессы в электрических системах. М.: Энергия, 1985, с. 530.
18. Виноградов А. Б. Учет потерь в стали, насыщения и поверхностного эффекта при моделировании динамических процессов в частотно-регулируемом асинхронном электроприводе// Электротехника, 2005, № 5, с. 57–61.
19. Вольдек А. И. Электрические машины. Л., “Энергия”, 1974.
20. Горелик Л. В. Расчет параметров короткозамкнутого ротора асинхронного двигателя в пусковых режимах. Электротехника, 1979, № 7, с. 24–25.
21. Грюнер А. И. Влияние магнитной цепи на электрические параметры ротора с глубокими пазами// Электричество, 1990, № 9.
22. Иванов – Смоленский А. В. Электрические машины. М., “Энергия”, 1980.
23. Инкин А. И. Электромагнитные поля и параметры электрических машин. Новосибирск, “ЮКЭА”, 2002.
24. Каваре Ясер Хусейн. Учет эффекта вытеснения тока в стержнях ротора асинхронного двигателя при его моделировании в среде Matlab// Наукові праці Донецького національного технічного університету. Серія: Електротехніка і енергетика, випуск 67: Донецьк: ДонНТУ, 2003, с. 160–162.
25. Казовский Е. Я. Исследование электромагнитных полей, параметров и потерь в мощных электрических машинах / Е.Я. Казовский, Я.Б. Данилевич. – Л.: Наука, 1966, с. 213.
26. Казовский Е. Я. Переходные процессы в электрических машинах переменного тока М.; Л.: Издательство АН СССР, 1962, с. 624.
27. Кетнер К. К. Переходные процессы в машинах переменного тока. Рига, РПИ, 1976.
28. Клоков Б. К. Расчет вытеснения тока в стержнях произвольной конфигурации// Электротехника, 1969, № 6, с. 25–29.
29. Клоков Б.К. Практические методы учета вытеснения тока// Электротехника, 1970, № 6, с. 48–51.
30. Копылов И. П. Проектирование электрических машин. М., “Энергия”, 1980.
31. Копылов И. П. Математическое моделирование электрических машин. М., “Высшая школа”, 1994.
32. Кравчик А. Э., Шлаф М. М., Афонин В. И., Соболенская Е. А. Асинхронные двигатели серии 4А. Справочник. М.: Энергоиздат, 1982. – 504 с. ил.
33. Мамиконянц Л. Г. Анализ некоторых аспектов переходных и асинхронных режимов синхронных и асинхронных машин М.: ЭЛЕКС-КМ, 2006.
34. Постников И. М. Обобщенная теория и переходные процессы электрических машин. М., “Высшая школа”, 1975.
35. Рюденберг Р. Явления неустановившегося режима в электрических установках, ГНТИ, 1931.
36. Рюденберг Р. Переходные процессы в электроэнергетических системах. М.; ИЛ, 1955, с. 714.
37. Сивокобыленко В. Ф., Павлюков В. А. Расчет параметров схем замещения и пусковых характеристик глубокопазных асинхронных машин// Электричество, 1979, № 10, с. 35–39.
38. Сивокобыленко В. Ф. Моделирование режимов работы асинхронных машин с учетом насыщения магнитных цепей и вытеснения токов в роторе// Наукові праці ДонНТУ, Серія Електротехніка і енергетика, Вип. 112. Донецьк: ДонНТУ, 2006, с. 10–16.

39. Соколов М. М., Петров Л. П., Масандилов Л. Б., Ладензон В. А. Электромагнитные переходные процессы в асинхронном электроприводе. М., “Энергия”, 1967.
40. Соломин А. В. Учет влияния вытеснения тока на параметры проводника обмотки тягового линейного асинхронного двигателя при его произвольном расположении по высоте паза// Вестник Ростовского государственного университета путей сообщения, 2000, №1, с. 30–35.
41. Соломин В.А., Замшина Л.Л. Параметры регулируемого тягового линейного асинхронного двигателя с учетом вытеснения тока в пазу// Вестник Ростовского государственного университета путей сообщения, 2000, № 2, с. 57-60.
42. Соломин А.В., Замшина Л. Л. Учет влияния вытеснения тока в стержне вторичного элемента линейного асинхронного двигателя при его произвольном расположении по высоте паза// Известия высших учебных заведений, Электромеханика, 2005, № 3, с. 34–37.
43. Ульянов С. А. Электромагнитные переходные процессы. М: Энергия, 1970, с. 520.
44. Фильц Р. В. Математические основы теории электромеханических преобразователей. Киев, “Наукова думка”, 1979.
45. Цуканов В. И, Фисенко В. Г. Методы расчета параметров обмотки ротора с учетом эффекта вытеснения тока// Труды МЭИ, 1980, вып. 449.
46. Цуканов В. И., Георгиади В. Х. Расчет на ЭВМ коэффициентов вытеснения токов в стержне ротора электрических машин// Электротехника, 1982, № 12.
47. Чабан В. И. К расчету переходных процессов в демпферных контурах электрических машин// Электричество, 1978, № 6.
48. Щербаков В. Г., Вольвич А. Г., Орлов Ю. А., Колпахчян П. Г. Оперативное определение нелинейных параметров асинхронного двигателя с короткозамкнутым ротором// Электротехника, 2009, № 8, с.22–26.
49. Янко-Триницкий А. А. Уравнения переходных электромагнитных процессов асинхронного двигателя и их решения// Электричество, 1951, № 3, с. 18–25.